Railway wheel failure caused by flange crack, part 1: Background and failure analysis

Downloaded from: https://research.chalmers.se, 2026-04-15 15:39 UTC

Citation for the original published paper (version of record):

Hjertsén, D., Ekberg, A., Vernersson, T. (2026). Railway wheel failure caused by flange crack, part 1: Background and failure analysis. Engineering Failure Analysis, 191. http://dx.doi.org/10.1016/j.engfailanal.2026.110770

N.B. When citing this work, cite the original published paper.

research.chalmers.se offers the possibility of retrieving research publications produced at Chalmers University of Technology. It covers all kind of research output: articles, dissertations, conference papers, reports etc. since 2004. research.chalmers.se is administrated and maintained by Chalmers Library

(article starts on next page)

Engineering Failure Analysis 191 (2026) 110770

Contents lists available at ScienceDirect

Engineering Failure Analysis

journal homepage: www.elsevier.com/locate/engfailanal

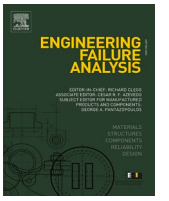

Railway wheel failure caused by flange crack, part 1: Background and failure analysis

David Hjertsén [a], Anders Ekberg [b,*], Tore Vernersson [b]

[a] Element Materials Technology, ASJ-vägen 7, SE 582 54 Linköping, Sweden
[b] CHARMEC, Chalmers University of Technology, SE 412 96 Gothenburg, Sweden

ARTICLE INFO

Keywords:
Railway
Derailment
Fatigue
Tread braking
Wheel fracture

ABSTRACT

A technical investigation is carried out on a railway wheel failure caused by a fatigue crack initiated at the inside of the flange. When the crack reached a critical size it propagated into the hub causing loss of grip on the axle and a shift inwards along the axle. Continued operations with the displaced wheel caused damage to 15 km of track.

The cracked wheel was at the end of its service life with wheel diameter and flange thickness close to limit values. Material testing shows requirements to be fulfilled. Fractographic and metallographic analyses establish how the final fracture progressed from initiation at the flange. The conclusions drawn in the current study provide input to a subsequent investigation of load conditions causing the failure which is presented in the second part of this paper [1].

1. Background

On the 17th of December 2023, several wagons of a fully loaded iron ore train derailed at Vassijaure station on route from Kiruna in Sweden to Narvik in Norway on the Iron Ore line. Investigations [2] revealed that at a position some fifteen km before the final derailment, one wheel was detached from the axle seat. Data from a wheel load measurement station located approximately 1 km beyond the location where the first damage in track is seen confirm that the damaged axle passed the station with one wheel on the rail and the other wheel inside the rail, however without any alarm being issued. This continued rolling inside the rail caused massive damage to rail, fastenings and sleepers, and secondary damage to the wheel. Finally, the wagon with the fractured wheel derailed in a switch causing additional derailment of some 12 wagons, see Fig. 1. As a consequence of the derailment, the line was closed for repair for two months, until 20 February 2024.

The failed wheel was put into service 31st October 2018, it operated in a test train with axle loads up to 32.5 tonnes (average load 31.0 tonnes) until October 2020. Since 29th June 2022 it was mounted on the wagon that eventually derailed. The total operating distance of the wheel at the time of failure was 528 000 km. The wheel was reprofiled at two occasions: March 2021 due to hollow wear and February 2022 due to thin flange. The flange back distance remained constant between these two reprofilings.

In the following it will be shown that the cause of the detached wheel can be linked to a radial fracture induced by a fatigue crack on the inside (towards centre of the track) of the flange and extending to the hub. This is a rare type of failure, only scarcely reported in the literature, see [3] and with only one similar case known from the Iron ore line in Sweden–Norway [2].

This failure type cannot really be characterised as rolling contact fatigue (cf. [4,5]) since the crack is not initiated/propagated in the

* Corresponding author.
E-mail address: anders.ekberg@chalmers.se (A. Ekberg).

https://doi.org/10.1016/j.engfailanal.2026.110770
Received 7 November 2025; Received in revised form 23 February 2026; Accepted 16 March 2026
Available online 18 March 2026
1350-6307/© 2026 The Author(s). Published by Elsevier Ltd. This is an open access article under the CC BY license (http://creativecommons.org/licenses/by/4.0/).

contact stress field but driven by cyclic tensile stresses on the inside of the flange (and promoted by tensile residual stresses due to flange overheating as shown in part 2 [1]). In that aspect, this type of fatigue failure is more akin to plain fatigue.

To further examine the occurrence of cracks on the inside of the flange non-destructive testing was carried out on the opposite wheel in the axle, and on wheels of the same kind reaching the end of operational life as discussed in section 5.

The detailed investigations to establish the characteristics and cause of the failure are reported in the following. The presentation sets out with an evaluation of fracture characteristics, examines geometry of wheel and brake block, reports material and mechanical test results. The current study provides input to an assessment of which load conditions that triggered fatigue initiation, crack growth and final fracture. These investigations that feature mechanical and thermomechanical FE analyses combined with fatigue and fracture analyses are reported in the second part of this paper [1]. Some main conclusions drawn in part 2 are that for the studied wheel profile hard flange contact in combination with residual tensile stresses from flange overheating cause sufficiently high stress levels to initiate crack growth from scratches on the inside of the flange and cause final fracture. It was further made likely that the crack started growing before the last reprofiling, which would correspond to a crack growth life (from a depth of around 3 mm) of at least 21 months.

The novel features of the study include the detailed assessment of this rare type of failure, and the combination of fractography, material testing, and numerical simulations to identify a likely failure scenario to establish root causes of this costly accident, in a setting where many parameters are uncertain and results are sensitive to small changes in the input set-up.

2. Fracture characteristics

During inspections after the derailment, it was found that the cracked wheel had shifted along the wheel axle from its original shrink-fitted position, see Fig. 2. This movement occurred while the train was running as a consequence of the loss of interference grip between wheel hub and axle seat.

Fig. 3 shows all salvaged parts of the wheel restored in their approximate original position with only minor parts missing. Yellow arrows show directions of fractures. The dashed yellow line indicates a crack branch not leading to fracture.

In the radius between the wheel rim and the web, blue colour shift from thermal oxides is noted and marked with a red arrow in Fig. 3. The blueing is an indication of previous exposure to a significantly elevated temperature and is found on both sides of the wheel. In addition, the other wheel on the axle also shows signs of heat damage in the corresponding position. The blueing colour can be linked to an elevated temperature. However, that would require knowledge on accessible oxygen (this part of the wheel is painted which can influence the oxidation) and time at the elevated temperature [6]. These parameters are not known in the current study.

The fracture surface in position 1 is considered to be the crack triggering final failure. As seen in Fig. 4, it consists of a fatigue crack initiated on the inside of the flange. Secondary damage to the crack in position 1 made further examinations in SEM futile for this crack. The crack geometry in Fig. 4 is employed in analyses and simulations in part 2 [1].

A fatigue crack was also found in position 2 in Fig. 3, see Fig. 5. This crack was examined in SEM both on replica and on the fracture surface. The examination did not contribute any further information regarding growth rate etc. due to the lack of finer fractographic characteristics. It was however clear that the area outside the fatigue crack is dominated by cleavage fracture. The fracture from the crack in position 2 is considered to be secondary based on crack propagation directions and connections.

Casting with a replica (Struers Repliset) was used to allow examination of the area in the hub close to the axle (indicated by light blue arrow in Fig. 3) without extensive cutting. This examination showed that the crack did not originate inside the hub, but grew towards the hub, see Fig. 6. SEM investigations in the area confirms the presumed fracture direction, see Fig. 6b and reveals that the crack is dominated by transcrystalline cleavage fracture which indicates a brittle overload fracture.

The crack starting at position 3 had severe damage. However, no signs of any other fracture mechanism than brittle overload was found. It was therefore assessed to be a secondary crack.

Fig. 1. The wagon with the fractured wheel to the left. Note the detached bogie where also the wheelset with the fractured wheel is detached (red arrow). The travel direction is indicated by the yellow arrow. Picture CCBY 2.5 SE, Statens haverikommission [2].

Fig. 2. The fractured wheel shifted along the axle.

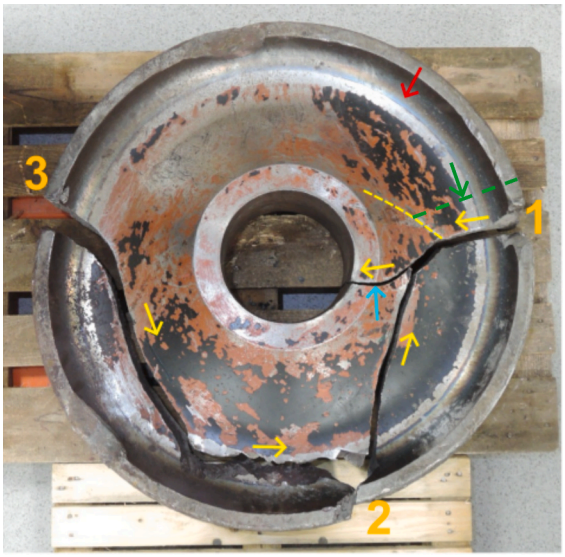

Fig. 3. The fractured wheel restored from salvaged parts. Yellow arrows show fracture directions, dashed yellow line a non-fracturing crack branch. Red arrow points at blue colour shift, light blue arrow indicates position of replica casting. Green dashed line and arrow show approximate position and direction of view of cross section in figures 7, 8 and 10.

Fig. 4. Fracture in position 1 of figure 2 with primary fatigue crack in flange indicated.

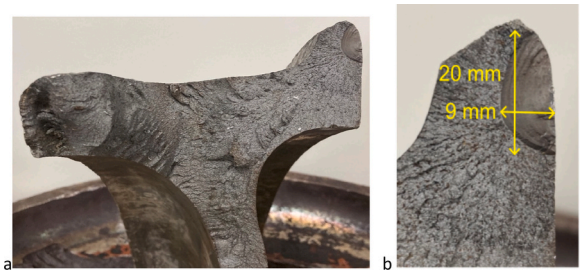

Fig. 5. Fracture in position 2 of figure 3. a) Overview of fracture surface. b) Detailed view of the fatigue crack.

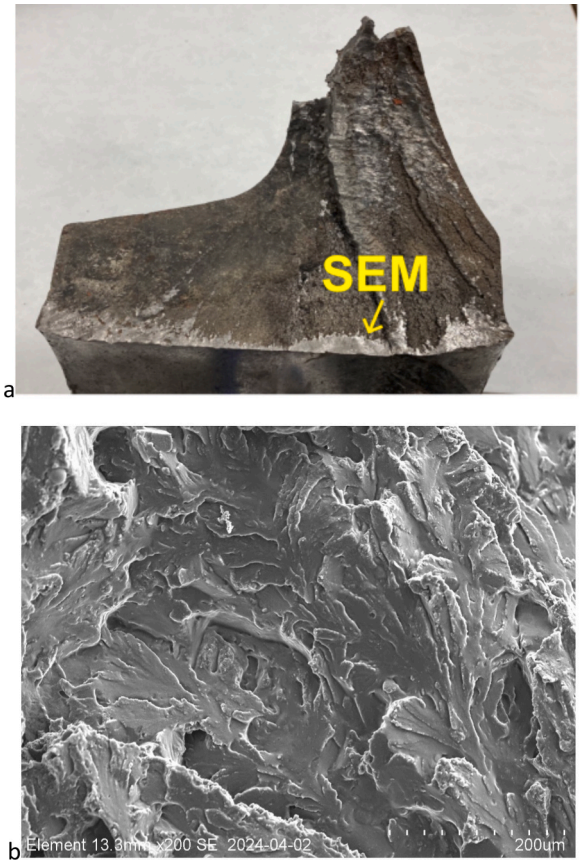

Fig. 6. a) replica of fracture area at the hub (position indicated by light blue arrow in figure3), web upwards. b) SEM picture at position indicated by yellow arrow in figure 6a, hub upwards.

3. Wheel rim and brake block profiles

As mentioned, the wheel rim on the fractured wheel was reprofiled. In addition, it was worn due to operational service but also as a consequence of rolling in ballast and impacting sleepers after detaching from the wheel seat. To measure remaining rim thickness on parts cut out for strength tests, caliper measurements and image analyses were used, see Fig. 7. The rim thickness is not entirely well defined in the maintenance instructions but is estimated to be between 33.0 and 33.5 mm after the accident. This gives a margin to the allowed minimum wheel diameter after reprofiling of less than 5 mm, and some 8–9 mm margin to the minimum allowed wheel diameter in operation.

The measured tread wear corresponds to up to 1 mm since the last reprofiling 21 months before derailment. This is not entirely consistent with the wear rate between the two previous turnings, which was 0.9 mm in 11 months. The discrepancy is interpreted primarily as a consequence of the measurement of rim thickness not being as reliable as diameter measurements. Regardless, the rim thickness is close to its limit value.

Also flange thickness, flange height and q_r (essentially flange slope) on the damaged wheel were measured in a cross section, see

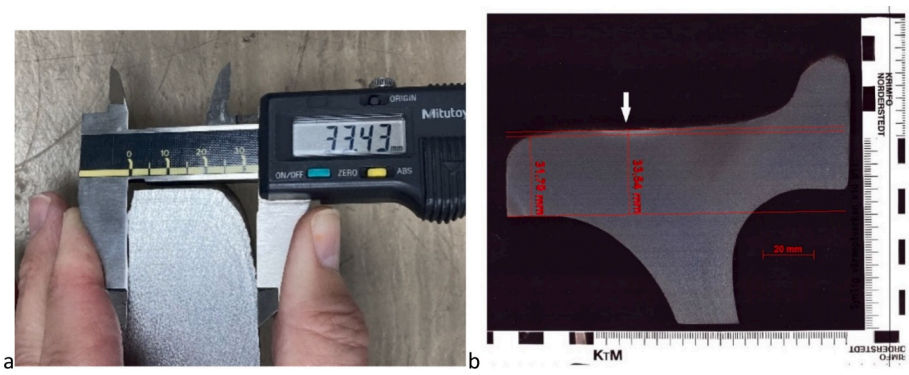

Fig. 7. a) rim thickness measurement using a caliper, and b) wheel rim dimensions from image analysis.

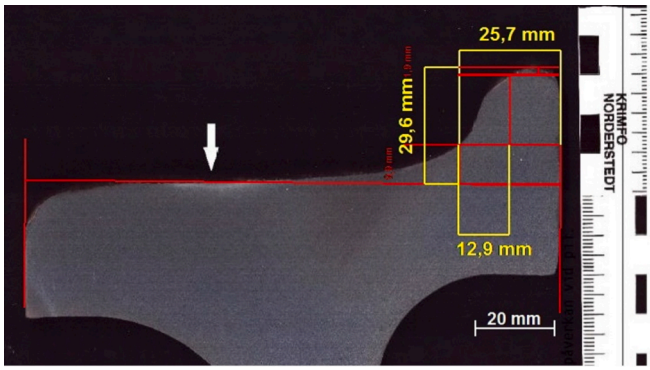

Fig. 8. Flange thickness (25.7 mm), height (29.6 mm) and q_r (12.9 mm).

Fig. 8. Flange height and (especially) q_r are dependent on the secondary damage to the flange top which was very exposed when rolling in ballast and impacting sleepers. These values are therefore not necessarily reflecting conditions before derailment. Regarding the flange thickness, which should be less influenced by the derailment, it is found to be small but above the minimum allowed dimension of 22 mm.

The Iron Ore wagons use so-called push-brakes and 1xBg brake block configurations. A single sinter brake block is used at each wheel. Two brake blocks found at the accident site were visually examined. One brake block was found at post 115, where damage to the track begins to appear. This brake block shows signs of having been heavily worn against the wheel flange during braking. It also has uneven wear along the length, see Fig. 9. The latter is not uncommon and relates to the mounting configuration of the brake block holder [7]. It has not affected the failure conditions but is commonly considered a maintenance issue since it increases brake shoe consumption.

4. Mechanical and material testing

Key mechanical testing results for the investigated wheel produced from AAR grade B material are provided in Table 1. The material fulfils the AAR grade B specifications.

For comparison, some values are also contrasted to requirements for ER9 according to EN 13262:2020. The ER9 is the highest strength class according to the EN standard and has a similar composition, but slightly lower carbon content than what is specified for the investigated wheel.

The tensile strength of the investigated wheel steel is in line with the requirements for ER9, deviations when it comes to strength are essentially expected given that the test position is shifted in relation to the original tread.

The impact toughness is only informative in the material specification for the investigated wheel. Values are found to be low compared to the ER9 standard. The impact test was however carried out in a test position 15 mm below the surface of the cracked wheel, which is about 25 mm closer to the centre of the wheel than the position used when testing a new wheel. Since the impact strength varies with distance from the original surface, the results reflect a difference related to the test position. Further, they reflect the high hardness imposed to improve wear resistance.

The chemical composition analysis is presented in Table 2. In general, the steel does not deviate from the specification. There is a small deviation in carbon content between the material certificates and test results that has not been explained but is considered reasonable and likely linked to sample extraction, testing methodology, and the influence of operations.

Fig. 9. Brake block found where track damage begun. a) Longitudinal profile. b) Transverse profile matched towards the opposite wheel on the axle. c) Less worn brake block from another wagon.

Table 1
Mechanical testing results and values stipulated for material ER9.

Strength parameter	Test value	ER9	Strength parameter	Test value	ER9
Fracture stress (tread) [MPa]	979	900–1050	Impact toughness RT, KU average value [J]	7.2	≥13
Fracture stress (body) [MPa]	845	≤849[a]	Impact toughness RT, KU min value [J]	5.4	≥9
Yield strength (raceway) [MPa]	548	–	Impact toughness –20 °C KV average [J]	4.5	≥8
Yield strength (body) [MPa]	438	≥350	Impact toughness –20 °C KV min value [J]	4.2	≥5
Fracture strain (tread) [%]	15.5	≥12	Impact toughness –40 °C KV average [J]	3.5	–
Fracture strain (body) [%]	16.5	≥14	Impact toughness –20 °C KV min value [J]	2.5	–

[a] Reduction of at least 130 MPa is required as compared to rim of same wheel.

Table 2
Composition analysis [weight %].

C	Si	Mn	P	S	Cr
0.60	0.35	0.84	0.007	0.001	0.10
Cu	Mo	Ni	V	Cr + Mo + Ni	
0.18	0.03	0.11	0.043	0.24	

In order to perform the examination of the microstructure and the hardness measurement the cross section was cut into six samples as indicated by the blue lines in Fig. 10. These samples were ground and polished down to 0.03 μm using standard metalographical methods and etched in Nital 2% for the microstructural examination.

Hardness values presented in Fig. 10 are in good agreement with batch certificate values from the manufacturer measured at corresponding positions. Note that in the radii where bluing is noted (see Fig. 3), there is a marginal decrease in hardness towards the surface. This is likely due to annealing related to the heat event that caused the blueing.

Regarding the microstructure, there were no deviations from the expected ferrite/pearlitic microstructure with a deformation zone

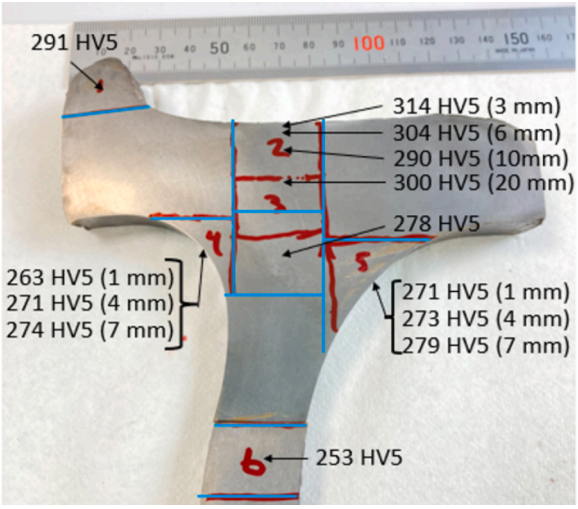

Fig. 10. Hardness mapping of the wheel cross section. Blue lines mark the location of the six micro-sections, reported values are averages of three hardness tests at indicated depth below surface.

under the tread. No extensive martensitic structure is found under the tread.

5. Non-destructive testing

Investigations of the inside of the flange on the wheel mounted opposite the fractured wheel revealed scratches on the inside of the flange, see Fig. 11 However, no larger crack-like defects were found.

Scratches on the inside of the flange as seen in Fig. 11 is a common type of damage but not commonly known to cause propagating fatigue cracks. To investigate further, ten wheels at the end of their operational life were examined using magnetic particle inspection to detect any cracking on the inside of the flange. No large cracks were found, however microcracks extending in the radial direction are present to varying degrees on four wheels, see example in Fig. 12. There was however no clear relationship between crack formation and total operating distance, distance since the last re-turning, or wheel diameter.

Fig. 11. a) inside of flange on the wheel opposite the fractured wheel. b) detail of radial scratch pattern on inside of flange. Pictures taken during testing with red penetrant.

Fig. 12. Magnetic particle inspection showing indications of microcracks on the inside of the flange.

6. Concluding remarks

The investigations carried out together with the existence of a previous similar case strengthen the hypothesis that the failure started with fatigue crack initiation at the inside of the flange. The crack grew until it reached a critical size where the final fracture developed with one branch of the crack extending into the hub. This caused the wheel to lose its grip after which the wheel moved along the axle. The continued rolling inside the rail caused secondary damage to the wheel.

As mentioned, this type of wheel damage/damage mechanism is very unusual and requires a loading that imposes (cyclic) tensile stresses at the inside of the flange. In addition to the current failure, the authors are aware of one similar case on the Iron Ore line [2]. This wheel fracture happened on a wheel that had a known brake malfunctioning event three years prior while the train was standing in Narvik. The loading at fracture had to be quasistatic from cooling of the wheel that had been heated in the descent to Narvik. The stress magnitudes at that occasion should therefore be much lower than for the current wheel fracture, which is in line with the critical crack size that was found to cover more or less the entire flange area, thus much larger than in the current case.

Fatigue cracks initiating on the top/inside of the flange are also mentioned in reference [3]. They are characterised as thermal cracks. Thermal cracks in general form during tread braking by yielding of the heated material when the restricted thermal expansion causes compressive thermal stresses. If the stress levels are sufficiently high, there will be plastic deformation resulting in tensile residual stresses at cooling after braking. If the tensile residual stresses that mainly act in circumferential direction are sufficiently high, they may cause (quasistatic) crack growth in the radial direction, see [8]. In railway wheels, such so-called thermal cracks can range in size from parts of millimetres to extending all the way from tread to the hub. In reference [3], fatigue cracks initiating on the top/inside of the flange are stated to be very rare since the introduction of rim quenching, i.e. the wheel is chilled after heating, which introduces compressive residual stresses in the wheel rim and also higher hardness, see [9,10]. The compressive residual stresses and the hardness gradually decrease with depth from the tread and are replaced by tensile residual stress in the web/disk (to preserve equilibrium). In a compilation of causes of wheel failures in America between 1995 and 2015 referenced in [3] there is no case classified as fatigue cracks initiating on the top/inside of the flange out of 250 to 350 wheel failures annually.

In [11] back rim cracks are discussed. It is stated that these in most cases are initiated at rim stamping and are due to retarder shoe and/or guard rail action. In the current case there is no rim stamping. The standard EN 15313:2024 also mentions radial marks on the inside of the rim. According to the standard they are permitted unless they 'exhibit a notch effect' or are 'associated with the presence of thermal effects at the rim–web transition'.

Fatigue cracking at the inside of the flange is not considered in the dimensioning of wheels according to the European standard EN 13979–1. This is reasonable for wheels in general as this type of damage does not appear to occur at all in the general wheel population. On the Iron Ore line with heavy haul traffic only two cases have been identified, which makes it extremely unusual also under these conditions. However, the consequences of the derailment were so severe that it justified a further investigation into load conditions causing the failure. These investigations, reported in part 2 of this study [1], draw on conclusions from the current study, which include.

- A blueing is noted on the wheel disc. This confirms that the wheel has been overheated by tread braking at some point. It cannot be excluded that this is secondary damage (heating after the wheel has been released from the axle). However, it is difficult to envision a scenario that creates such heat after the wheel has lost its grip on the axle. That there were signs of overheating also on the opposite wheel which only derailed in the Vassijaure station further supports that the wheel overheating should not have taken place between the derailment of the fractured wheel and the final derailment of the train in Vassijaure. It can be noted that no similar heat damage was reported in the similar case that occurred earlier on the Iron Ore line. However, in that case the fatigue crack was much larger and extended over almost the entire flange.

- A rough surface with radial scratches from operation is noted on the inside of flange of the opposite wheel on the axle. Such excessive surface roughness would promote crack initiation.
- Microcracks noted on wheels taken out of operation indicate that a cyclic stress in the circumferential direction can occur on the inside of the flange. This cyclic stress is likely to be caused by mechanical loading since the thermal loading relates to much fewer load cycles and thus requires the formation of plastic deformations to cause (low cycle) fatigue.
- Material testing has been performed. No deviations from requirements were found.
- The cracked wheel is at the end of its service life. The rim thickness is small with only some 5–6 mm of material remaining to the minimum permitted wheel diameter. Also the flange width is small (around 26 mm measured on the damaged profile) but above the requirement of at least 22 mm.

CRediT authorship contribution statement

David Hjertsén: Writing – review & editing, Methodology, Investigation, Conceptualization. **Anders Ekberg:** Writing – original draft, Investigation. **Tore Vernersson:** Writing – review & editing.

Declaration of competing interest

The authors declare that they have no known competing financial interests or personal relationships that could have appeared to influence the work reported in this paper.

Acknowledgements

The work is part of the activities within the CHARMEC centre of excellence in railway mechanics (www.chalmers.se/charmec). Parts of the research is funded by the Swedish Accident Investigation Authority, and parts under the European Union's Horizon Europe research and innovation programme under grant agreement No: 101102009 (TRANS4M-R).

Data availability

No data was used for the research described in the article.

References

[1] Anders Ekberg, Tore Vernersson, David Hjertsén, Railway wheel failure caused by flange crack, Part 2: Fatigue and fracture assessment (2025) In review.
[2] Jonas Bäckstrand, Mikael Hillbo, Lars Dahlin, Urspårning med godståg 9914 på Malmbanan (in Swedish: Derailment with freight train 9914 on the Iron Ore Line) (2025), The Swedish Accident Investigation Authority. https://shk.se/sok-utredningar/sparbunden-trafik/2023-12-20-ursparning-med-godstag-9914-pa-malmbanan.
[3] Matthew Dick, Narayana Sundaram, Eric Sherrock, Wheel failure investigation program: Phase I (2021) United States. Department of Transportation. Federal Railroad Administration. https://rosap.ntl.bts.gov/view/dot/54652.
[4] Eric E Magel, Rolling contact fatigue: a comprehensive review (2011) US Department of Transportation, Federal Railroad Administration, Technical report DOT/FRA/ORD-11/24. https://railroads.dot.gov/sites/fra.dot.gov/files/fra_net/89/TR_Rolling_Contact_Fatigue_Comprehensive_Review_final.pdf.
[5] Anders Ekberg, Bengt Åkesson, Elena Kabo, Wheel/rail rolling contact fatigue–Probe, predict, prevent, Wear 314 (1-2) (2014) DOI: 10.1016/j.wear.2013.12.004.
[6] Hubertus Colpaert, Metallography of steels - Interpretation of structure and the effects of processing - 10.4.5 Tempering colors. ASM International (2018). Retrieved from https://app.knovel.com/hotlink/pdf/id:kt011QKHM4/metallography-steels/tempering-colors.
[7] Sergii Panchenko, Juraj Gerlici, Alyona Lovska, Vasyl Ravlyuk, Ján Dižo, Miroslav Blatnickỳ, Analysis of asymmetric wear of brake pads on freight wagons despite full contact between pad surface and wheel, Symmetry 16 (3) (2024) DOI: 10.3390/sym16030346.
[8] Sara Caprioli, Tore Vernersson, Anders Ekberg, Thermal cracking of a railway wheel tread due to tread braking–critical crack sizes and influence of repeated thermal cycles, Proc. Inst. Mech. Eng., Part F: J. Rail Rapid Transit 227 (1) (2013), https://doi.org/10.1177/0954409712452347.
[9] EN 13262 Railway applications – Wheelsets and bogies - Wheels - Product requirements, CEN, Brussels, Belgium (2020).
[10] Jeff Gordon, A Benjamin Perlman, Estimation of residual stresses in railroad commuter car wheels following manufacture, U.S. Department of Transportation (2001)https://rosap.ntl.bts.gov/view/dot/8521.
[11] Britto R Rajkumar, Dan H Stone, Wheel failure mechanisms of railroad cars (1987) Association of American Railroads. https://railroads.dot.gov/sites/fra.dot.gov/files/fra_net/15043/Wheel_Failure.pdf.